40

On a Domain Embedding Method for Flow around Moving Rigid Bodies

R. Glowinski, T.-W. Pan, and J. Périaux

1 Introduction

Several applications lead to the numerical simulation of incompressible viscous flow around moving rigid bodies; let us mention for example blood flow around artificial heart valves. In this article we consider only the case where the rigid body motions are known a priori; the more complicated case where the rigid body motions are caused by hydrodynamical forces, among other forces, will be discussed in a forthcoming article. Following an approach advocated — to our knowledge — by Peskin [Pes72] we use a *domain embedding* method (also called *fictitious domain method* by some authors) which consists of filling the moving bodies by the surrounding fluid and taking into account the boundary conditions on these bodies by introducing a well chosen distribution of boundary forces. In the particular case of the *Dirichlet boundary* conditions considered in this article it is quite convenient to use a *Lagrange multiplier* method which is well suited to the variational formulations commonly used to study the Navier-Stokes equations and their approximation, by finite element methods for example. Another important component of the solution method is a time discretization by operator splitting which reduces the simulation to a sequence of subproblems for which efficient solution methods exist already.

Figure 1. The flow region

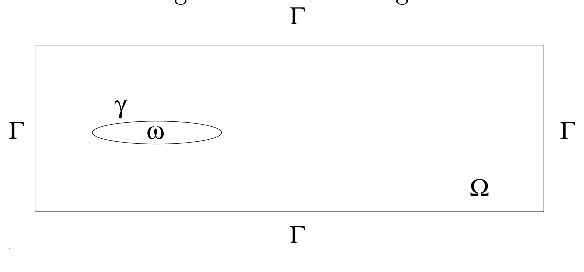

Ninth International Conference on Domain Decomposition Methods
Editor Petter E. Bjørstad, Magne S. Espedal and David E. Keyes

2 A Model Problem and its Lagrange Multiplier/Domain Embedding Formulation

The geometrical situation is as in Figure 1. With $\omega = \omega(t)$ a moving rigid body ($\omega \subset \Omega \subset \boldsymbol{R}^d$, d =2, 3), we consider for $t > 0$ the solution of the *Navier-Stokes equations*

$$\frac{\partial \mathbf{u}}{\partial t} - \nu \Delta \mathbf{u} + (\mathbf{u} \cdot \nabla)\mathbf{u} + \nabla p = \mathbf{f} \, in \, \Omega \setminus \overline{\omega(t)}, \tag{1}$$

$$\nabla \cdot \mathbf{u} = 0 \, in \, \Omega \setminus \overline{\omega(t)}, \tag{2}$$

$$\mathbf{u}(\mathbf{x}, 0) = \mathbf{u}_0(\mathbf{x}), \quad \mathbf{x} \in \Omega \setminus \overline{\omega(0)}, (with \, \nabla \cdot \mathbf{u}_0 = 0), \tag{3}$$

$$\mathbf{u} = \mathbf{g}_0 \, on \, \Gamma, \tag{4}$$

$$\mathbf{u} = \mathbf{g}_1 \, on \, \gamma(t). \tag{5}$$

In (1)-(5) $\mathbf{u}$ and p denote, as usual, the *velocity* and *pressure*, respectively; $\nu(> 0)$ is the *viscosity*, $\mathbf{f}$ the density of external forces, $\mathbf{x}$ the generic point of $\boldsymbol{R}^d$ ($\mathbf{x} = \{x_i\}_{i=1}^d$), $\gamma(t) = \partial\omega(t)$ and $(\mathbf{u} \cdot \nabla)\mathbf{u} = \{\sum_{j=1}^d u_j \frac{\partial u_i}{\partial x_j}\}_{i=1}^d$. We suppose that $\mathbf{g}_1$ is the velocity on $\gamma(t)$ of the rigid body $\omega(t)$ which implies that $\int_{\gamma(t)} \mathbf{g}_1 \cdot \mathbf{n} \, d\gamma = 0$, and that $\int_\Gamma \mathbf{g}_0 \cdot \mathbf{n} \, d\Gamma = 0$. In the following, we shall use, if necessary, the notation $\phi(t)$ for the function $\mathbf{x} \to \phi(\mathbf{x}, t)$.

We introduce first the functional spaces $\mathbf{V}_{\mathbf{g}_0(t)} = \{\mathbf{v} | \mathbf{v} \in (H^1(\Omega))^d, \mathbf{v} = \mathbf{g}_0(t) \, on \, \Gamma\}$, $\mathbf{V}_0 = (H_0^1(\Omega))^d$, $L_0^2(\Omega) = \{q | q \in L^2(\Omega); \int_\Omega q \, d\mathbf{x} = 0\}$ and $\Lambda(t) = (\mathbf{H}^{-1/2}(\gamma(t)))^d$. With $\tilde{\mathbf{f}}$ an L^2-lifting of $\mathbf{f}$ in Ω (we can take $\tilde{\mathbf{f}}|_{\overline{\omega(t)}} = \mathbf{0}$) and $\nabla \cdot \mathbf{U}_0 = 0$ ($\mathbf{U}_0|_{\Omega\setminus\overline{\omega(0)}} = \mathbf{u}_0$), it can be shown — at least formally — that problem (1)-(5) is *equivalent* to

For $t \geq 0$, *find* $\{\mathbf{U}(t), P(t), \lambda(t)\} \in \mathbf{V}_{\mathbf{g}_0(t)} \times L_0^2(\Omega) \times \Lambda(t)$ *such that*

$$\int_\Omega \frac{\partial \mathbf{U}}{\partial t} \cdot \mathbf{v} \, d\mathbf{x} + \nu \int_\Omega \nabla \mathbf{U} \cdot \nabla \mathbf{v} \, d\mathbf{x} + \int_\Omega (\mathbf{U} \cdot \nabla)\mathbf{U} \cdot \mathbf{v} \, d\mathbf{x} - \int_\Omega P \nabla \cdot \mathbf{v} \, d\mathbf{x}$$
$$= \int_\Omega \tilde{\mathbf{f}} \cdot \mathbf{v} \, d\mathbf{x} + \int_{\gamma(t)} \lambda \cdot \mathbf{v} \, d\gamma, \, \forall \mathbf{v} \in \mathbf{V}_0, \tag{6}$$

$$\int_\Omega q \nabla \cdot \mathbf{U}(t) \, d\mathbf{x} = 0, \ \forall q \in L^2(\Omega), \tag{7}$$

$$\int_{\gamma(t)} (\mathbf{U}(t) - \mathbf{g}_1(t)) \cdot \mu \, d\gamma = 0, \ \forall \mu \in \Lambda(t), \tag{8}$$

$$\mathbf{U}(0) = \mathbf{U}_0 \ in \ \Omega, \quad \mathbf{U} = \mathbf{g}_0 \ on \ \Gamma, \tag{9}$$

in the sense that $\mathbf{U}(t)|_{\Omega\setminus\overline{\omega(t)}} = \mathbf{u}(t)$ and $P(t)|_{\Omega\setminus\overline{\omega(t)}} = p(t)$. We can easily show that $\lambda = [\nu \partial \mathbf{U}/\partial \mathbf{n} - \mathbf{n}P]_\gamma$, where $[\ ]_\gamma$ denotes the *jump* at γ.

Remark 2.1: The mathematical analysis of flow problems such as (1)-(5) is addressed in, e.g., [AG93] (see also the references therein).

Remark 2.2: We observe that the *actual geometry*, i.e., $\omega(t)$ and $\gamma(t)$ occurs "only" in the $\gamma(t)$-integral in (6) and in (8); this is a justification of the domain embedding approach.

3 Finite Element Approximation of Problem (6)-(9)

Figure 2. Part of the triangulation of Ω with mesh points indicated by "$*$" on the disk boundary

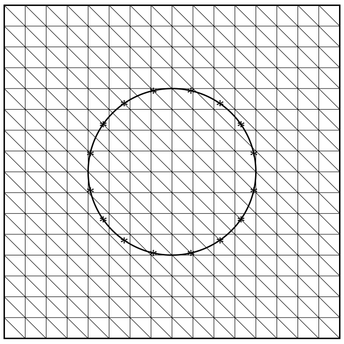

We suppose that $\Omega \subset \boldsymbol{R}^2$ $(d = 2)$. With h a space discretization step we introduce a *finite element* triangulation $\mathcal{T}_h$ of $\overline{\Omega}$ and then $\mathcal{T}_{h/2}$ a triangulation twice finer obtained by joining the midpoints of the edges of $\mathcal{T}_h$. We define then the following finite dimensional spaces which approximate $\mathbf{V}_{\mathbf{g}_0}$, $\mathbf{V}_0$, $L^2(\Omega)$, $L_0^2(\Omega)$ respectively

$$\mathbf{V}_{\mathbf{g}_{0h}} = \{\mathbf{v}_h | \mathbf{v}_h \in C^0(\bar{\Omega})^2,\, \mathbf{v}_h|_T \in P_1 \times P_1,\, \forall T \in \mathcal{T}_h,\, \mathbf{v}_h|_\Gamma = \mathbf{g}_{0h}\}, \tag{10}$$

$$\mathbf{V}_{0h} = \{\mathbf{v}_h | \mathbf{v}_h \in C^0(\bar{\Omega})^2,\, \mathbf{v}_h|_T \in P_1 \times P_1,\, \forall T \in \mathcal{T}_h,\, \mathbf{v}_h|_\Gamma = \mathbf{0}\}, \tag{11}$$

$$L_h^2 = \{q_h | q_h \in C^0(\bar{\Omega}),\, q_h|_T \in P_1,\, \forall T \in \mathcal{T}_{2h}\},\, L_{0h}^2 = \{q_h | q_h \in L_h^2,\, \textstyle\int_\Omega q_h\, d\mathbf{x} = 0\}; \tag{12}$$

in (10)-(12), P_1 is the space of the polynomials in x_1, x_2 of degree ≤ 1 and $\mathbf{g}_{0h}$ is an approximation of $\mathbf{g}_0$ such that $\int_\Gamma \mathbf{g}_{0h} \cdot \mathbf{n}\, d\Gamma = 0$. Concerning the space $\Lambda_h(t)$ approximating $\Lambda(t)$, we define it by

$$\begin{aligned}\Lambda_h(t) = \{\mu_h | \mu_h \in (L^\infty(\gamma(t)))^2, \mu_h \text{ is constant on the arc joining} \\ 2 \text{ consecutive mesh points on } \gamma(t)\}.\end{aligned} \tag{13}$$

A particular choice for the mesh points on γ is visualized on Figure 2, where ω is a disk. Let us resist any requirement that the mesh points on γ have to be at the intersection of γ with the triangle edges of $\mathcal{T}_{h/2}$; (see [GG95] for more details and the relations between h_Ω and h_γ). This kind of decoupling between the Ω and γ meshes makes the domain embedding approach attractive for problems with moving boundaries like those discussed in this note. With the above spaces it is natural to approximate problem (6)-(9) by (with obvious notation)

$$\begin{aligned}\int_\Omega \frac{\partial \mathbf{U}_h}{\partial t} \cdot \mathbf{v}\, d\mathbf{x} + \nu \int_\Omega \nabla \mathbf{U}_h \cdot \nabla \mathbf{v}\, d\mathbf{x} + \int_\Omega (\mathbf{U}_h \cdot \nabla)\mathbf{U}_h \cdot \mathbf{v}\, d\mathbf{x} - \int_\Omega P_h \nabla \cdot \mathbf{v}\, d\mathbf{x} \\ = \int_\Omega \tilde{\mathbf{f}}_h \cdot \mathbf{v}\, d\mathbf{x} + \int_{\gamma(t)} \lambda_h \cdot \mathbf{v}\, d\gamma,\, \forall \mathbf{v} \in \mathbf{V}_{0h},\, \mathbf{U}_h(t) \in \mathbf{V}_{\mathbf{g}_0(t)h},\end{aligned} \tag{14}$$

$$\int_{\Omega} q\nabla \cdot \mathbf{U}_h(t)\, d\mathbf{x} = 0,\ \forall q \in L_h^2,\ P_h(t) \in L_{0h}^2, \tag{15}$$

$$\int_{\gamma(t)} (\mathbf{U}_h(t) - \mathbf{g}_1(t)) \cdot \mu\, d\gamma = 0,\ \forall \mu \in \Lambda_h(t),\ \lambda_h(t) \in \Lambda_h(t), \tag{16}$$

$$\mathbf{U}_h(0) = \mathbf{U}_{0h}; \tag{17}$$

in (17), $\mathbf{U}_{0h}$ is an approximation of $\mathbf{U}_0$, approximately divergence-free.

Figure 3.

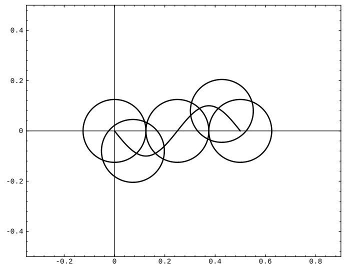

4 Time Discretization of (14)-(17) by Operator Splitting Methods

From an abstract point of view problem (14)-(17) is a particular case of the following class of initial value problems

$$\frac{d\phi}{dt} + A_1(\phi) + A_2(\phi) + A_3(\phi) = f,\ \ \phi(0) = \phi_0, \tag{18}$$

where the operators A_i can be *multivalued.* Among many operator splittings which can be employed to solve (18) we advocate the very simple one below (analyzed in, e.g., [Mar90]); it is only first-order accurate but its low order accuracy is compensated by good stability and robustness properties.

A fractional step scheme à la Marchuk-Yanenko: With $\triangle t$ a time discretization step and the initial guess, $\phi^0 = \phi_0$, the scheme is defined as follows:

For $n \geq 0$, *we obtain* ϕ^{n+1} *from* ϕ^n *via the solution of*

$$(\phi^{n+j/3} - \phi^{n+(j-1)/3})/\triangle t + A_j(\phi^{n+j/3}) = f_j^{n+1}, \tag{19}$$

with $j = 1, 2, 3$ and $\sum_{j=1}^{3} f_j^{n+1} = f^{n+1}$. Applying scheme (19) to problem (14)-(17) we obtain (with $0 \leq \alpha, \beta \leq 1$, $\alpha + \beta = 1$, and after dropping some of the subscripts h):

$$\mathbf{U}^0 = \mathbf{U}_{0h}; \tag{20}$$

for $n \geq 0$, we compute $\{\mathbf{U}^{n+1/3}, P^{n+1/3}\}$, $\mathbf{U}^{n+2/3}$, $\{\mathbf{U}^{n+1}, \lambda^{n+1}\}$ via the solution of

$$\begin{cases} \displaystyle\int_\Omega \frac{\mathbf{U}^{n+1/3} - \mathbf{U}^n}{\triangle t} \cdot \mathbf{v}\, d\mathbf{x} - \int_\Omega P^{n+1/3} \nabla \cdot \mathbf{v}\, d\mathbf{x} = 0,\ \forall \mathbf{v} \in \mathbf{V}_{0h}, \\ \displaystyle\int_\Omega q \nabla \cdot \mathbf{U}^{n+1/3}\, d\mathbf{x} = 0,\ \forall q \in L^2_h;\ \mathbf{U}^{n+1/3} \in \mathbf{V}^{n+1}_{\mathbf{g}_{0h}},\ P^{n+1/3} \in L^2_{0h}, \end{cases} \tag{21}$$

$$\begin{cases} \displaystyle\int_\Omega \frac{\mathbf{U}^{n+2/3} - \mathbf{U}^{n+1/3}}{\triangle t} \cdot \mathbf{v}\, d\mathbf{x} + \alpha\nu \int_\Omega \nabla \mathbf{U}^{n+2/3} \cdot \nabla \mathbf{v}\, d\mathbf{x} \\ \quad \displaystyle + \int_\Omega (\mathbf{U}^{n+1/3} \cdot \nabla) \mathbf{U}^{n+2/3} \cdot \mathbf{v}\, d\mathbf{x} = \alpha \int_\Omega \tilde{\mathbf{f}}^{n+1} \cdot \mathbf{v}\, d\mathbf{x},\ \forall \mathbf{v} \in \mathbf{V}_{0h}; \\ \mathbf{U}^{n+2/3} \in \mathbf{V}^{n+1}_{\mathbf{g}_{0h}}, \end{cases} \tag{22}$$

$$\begin{cases} \displaystyle\int_\Omega \frac{\mathbf{U}^{n+1} - \mathbf{U}^{n+2/3}}{\triangle t} \cdot \mathbf{v}\, d\mathbf{x} + \beta\nu \int_\Omega \nabla \mathbf{U}^{n+1} \cdot \nabla \mathbf{v}\, d\mathbf{x} \\ \quad \displaystyle = \beta \int_\Omega \tilde{\mathbf{f}}^{n+1} \cdot \mathbf{v}\, d\mathbf{x} + \int_{\gamma^{n+1}} \lambda^{n+1} \cdot \mathbf{v}\, d\gamma,\ \forall \mathbf{v} \in \mathbf{V}_{0h}, \\ \displaystyle\int_{\gamma^{n+1}} (\mathbf{U}^{n+1} - \mathbf{g}^{n+1}_{1h}) \cdot \mu\, d\gamma = 0,\ \forall \mu \in \Lambda^{n+1}_h; \\ \mathbf{U}^{n+1} \in \mathbf{V}^{n+1}_{\mathbf{g}_{0h}} (= \mathbf{V}_{\mathbf{g}_0((n+1)\triangle t)h}),\ \lambda^{n+1} \in \Lambda^{n+1}_h (= \Lambda_h((n+1)\triangle t)). \end{cases} \tag{23}$$

5 Solution of the Subproblems (21), (22) and (23)

By inspection of (21) it is clear that $\mathbf{U}^{n+1/3}$ is the $L^2(\Omega)^2$-projection of $\mathbf{U}^n$ on the (affine) subset of the functions $\mathbf{v} \in \mathbf{V}^{n+1}_{\mathbf{g}_{0h}}$ such that $\int_\Omega q \nabla \cdot \mathbf{v}\, d\mathbf{x} = 0$, $\forall q \in L^2_h$, $P^{n+1/3}$ being the corresponding Lagrange multiplier in L^2_{0h}. The pair $\{\mathbf{U}^{n+1/3}, P^{n+1/3}\}$ is *unique* and to compute it we can use an Uzawa/conjugate gradient algorithm operating in L^2_{0h} equipped with the scalar product $\{q, q'\} \to \int_\Omega \nabla q \cdot \nabla q'\, d\mathbf{x}$. We obtain thus an algorithm preconditioned by the discrete equivalent of $-\Delta$ for the homogeneous Neumann boundary condition. Such an algorithm is *very* easy to implement and is described in [GPP96]; it seems to have excellent convergence properties.

If $\alpha > 0$, problem (22) is a classical one; it can be easily solved, for example, by a least squares/conjugate gradient algorithm like those discussed in [Glo84].

If $\beta > 0$ the solution of problem (23) has been discussed in [GPP94]. In the particular case where $\beta = 0$, problem (23) reduces to an $L^2(\Omega)^2$-projection over the subspace of $\mathbf{V}^{n+1}_{\mathbf{g}_{0h}}$ of the functions $\mathbf{v}$ satisfying the condition $\int_{\gamma^{n+1}} (\mathbf{v} - \mathbf{g}^{n+1}_{1h}) \cdot \mu\, d\gamma = 0$, $\forall \mu \in \Lambda^{n+1}_h$. It follows from the above observation that if $\beta = 0$, problem (23) can be solved by an Uzawa/conjugate gradient algorithm operating in Λ^{n+1}_h, which has many similarities with the algorithm used to solve problem (21). If one uses the trapezoidal rule to compute the various $L^2(\Omega)$-integrals in (23), taking $\beta = 0$ brings further simplification since in that particular case $\mathbf{U}^{n+1}$ will coincide with $\mathbf{U}^{n+2/3}$ at those vertices of $\mathcal{T}_{h/2}$ such that the support of the related shape function does not intersect γ^{n+1}; from the above observation it follows that to obtain $\mathbf{U}^{n+1}$ and λ^{n+1} we have to solve a linear system of the following form

$$A\mathbf{x} + B^t\mathbf{y} = \mathbf{b},\ \ B\mathbf{x} = \mathbf{c}. \tag{24}$$

For the numerical simulations presented in Section 6 we have used $\alpha = 1$ and $\beta = 0$ in (22), (23).

6 Numerical Experiments

We simulate a two-dimensional flow with $\Omega = (-0.35, 0.9) \times (-0.5, 0.5)$ (see Figure 3) and ω a moving disk of radius 0.125. The center of the disk is moving between $(0,0)$ and and $(0.5,0)$ along a prescribed trajectory $(x(t), y(t)) = (0.25(1 - \cos(\frac{\pi t}{2})), -0.1\sin(\pi(1-\cos(\frac{\pi t}{2}))))$ (see Figure 3) of period 4. Several different positions of the disk have been shown on Figure 3. The boundary conditions are $\mathbf{u} = \mathbf{0}$ on Γ and $\mathbf{u}$ on $\partial\omega(t)$ coinciding with the disk velocity. We suppose that the disk rotates counterclockwise at angular velocity 2π. Since we are taking $\nu = 0.005$, the maximum Reynolds number based on the disk diameter as characteristic length is 102.336. On Ω we have used a regular triangulation $\mathcal{T}_{h/2}$ to approximate the velocity, like the one in Figure 2, the pressure grid $\mathcal{T}_h$ being twice coarser. Concerning $\Lambda_h(t)$, $\gamma(t)$ has been divided into M subarcs of equal length. We have done two simulations: For the first one we have taken $h = 1/128$, $\triangle t = 0.00125$ and $M = 80$. For the second we have taken $h = 1/256$, $\triangle t = 0.00125$ and $M = 160$. With stopping criteria of the order of 10^{-12} we need around 10 iterations at most to have convergence of the conjugate gradient algorithms used to solve the problems at each step of the scheme (20)-(23). On Figure 4, we show the isobar lines, the vorticity density and the streamlines obtained at t =5, 6, 7, 8 for $h = 1/256$, $\triangle t = 0.00125$ and $M = 160$. There is a good agreement between the results obtained from these two simulations.

Acknowledgement

We would like to acknowledge the helpful comments and suggestions of E. J. Dean, J. W. He, H. H. Hu, D. D. Joseph, Y. Kuznetsov, B. Maury, A. H. Sameh and F. J. Sanchez, and the support of University of Houston and the Department of Computer Science, University of Minnesota. We also benefited from the support of NSF (Grants DMS 8822522, DMS 9112847, DMS 9217374), DRET (Grant 89424), DARPA (Contracts AFOSR F49620-89-C-0125 and AFOSR-90-0334), the Texas Board of Higher Education (Grants 003652156ARP and 003652146ATP), University of Houston (PEER grant 1-27682) and again NSF under the HPCC Grand Challenge Grant ECS-9527123.

REFERENCES

[AG93] Amiez G. and Gremaud P. A. (1993) On a penalty method for the navier-stokes problem in regions with moving boundaries. *Comp. Appl. Math.* 12: 113–122.

[GG95] Girault V. and Glowinski R. (1995) Error analysis of a fictitious domain method applied to a dirichlet problem. *Japan J. of Industrial and Applied Mathematics* 12: 487–514.

[Glo84] Glowinski R. (1984) *Numerical Methods for Nonlinear Variational Problems.* Springer-Verlag, New York.

Figure 4. Isobar lines (at left), vorticity density (at middle) and streamlines (at right) at time t =5, 6, 7, 8 in one period of disk motion. The disk moves from the left to the right, then to the left. The mesh size for velocity (resp., pressure) is $h = 1/256$ (resp., $h = 1/128$).

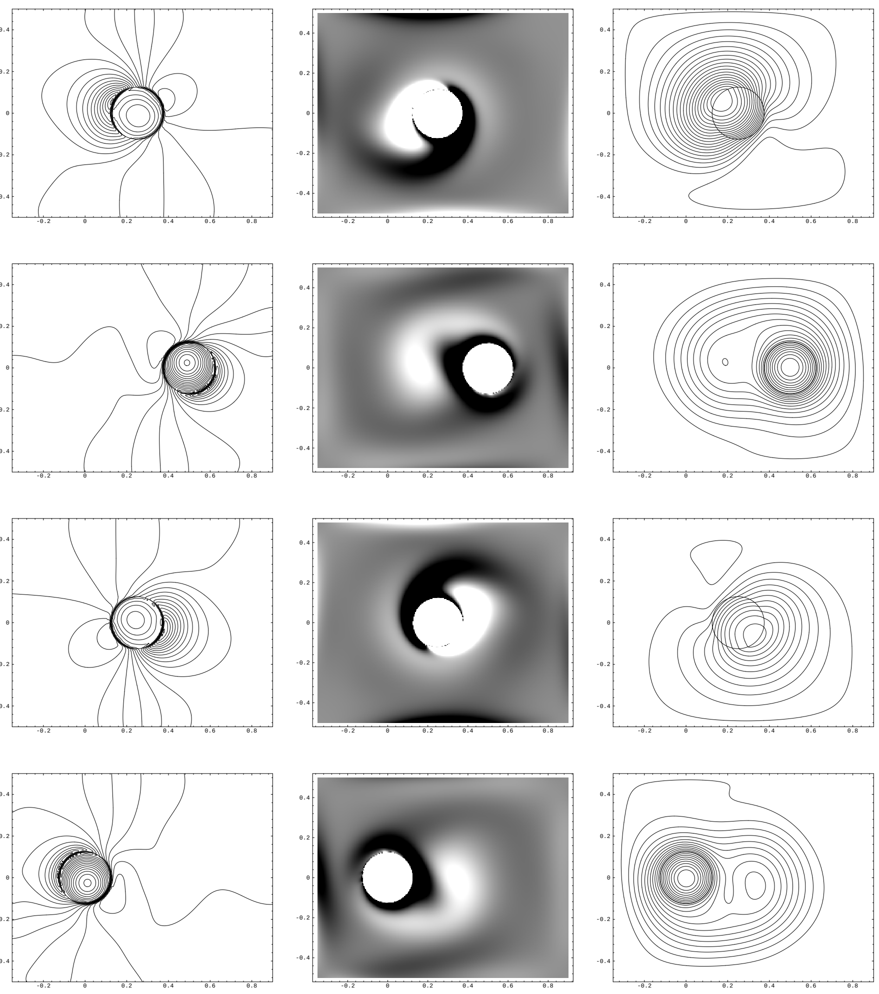

[GPP94] Glowinski R., Pan T. W., and Periaux J. (1994) A fictitious domain method for dirichlet problem and applications. *Comp. Meth. Appl. Mech. Eng.* 111: 283–303.
[GPP96] Glowinski R., Pan T. W., and Periaux J. (1996) Fictitious domain methods for incompressible viscous flow around moving rigid bodies. In *Proceedings of MAFELAP 1996 (to appear)*.
[Mar90] Marchuk G. I. (1990) Splitting and alternate direction methods. In Ciarlet P. and Lions J. (eds) *Handbook of Numerical Analysis*. Vol. I, North-Holland, Amsterdam.
[Pes72] Peskin C. Y. (1972) Flow patterns around heart valves: A numerical method. *J. Comp. Phys.* 10: 252–271.